Dynamics of interacting vesicles and rheology of vesicle suspension in shear flow

2008 EPL 82 58005

(http://iopscience.iop.org/0295-5075/82/5/58005)

A Letters Journal Exploring the Frontiers of Physics

June 2008

EPL, **82** (2008) 58005
doi: 10.1209/0295-5075/82/58005

www.epljournal.org

Dynamics of interacting vesicles and rheology of vesicle suspension in shear flow

V. Kantsler, E. Segre and V. Steinberg

Department of Physics of Complex Systems, Weizmann Institute of Science - Rehovot, 76100 Israel

received 28 January 2008; accepted in final form 15 April 2008
published online 29 May 2008

PACS 87.16.D- – Membranes, bilayers, and vesicles
PACS 47.61.-k – Micro- and nano- scale flow phenomena
PACS 47.63.-b – Biological fluid dynamics

Abstract – We studied the dynamics of isolated vesicles as well as vesicle interactions in semi-dilute vesicle suspensions subjected to a shear flow. We found that the long-range hydrodynamic interactions between vesicles give rise to strong fluctuations of vesicle shape and inclination angle, ϕ, though the functional dependence of ϕ and the transition path to tumbling motion is preserved. The dependence of the suspension viscosity on the viscosity ratio between inner and outer fluids, λ, was found to be non-monotonic and surprisingly growing with λ at the fixed outer fluid viscosity for $\lambda < 1$, at odds with recent predictions made for a dilute suspension of non-interacting vesicles.

Introduction. – Giant vesicles formed by a closed phospholipid bilayer membrane are widely used as a cell paradigm, and have potentially a number of applications as compartments for drugs or reacting chemicals that need to be brought to a specific target in micro-fluidic devices [1]. The growing interest in the dynamics of a single lipid vesicle freely suspended in a shear flow is reflected in numerous theoretical [2–6], numerical [7–9], and experimental [10–13] studies. The understanding of the single-vesicle dynamics was used as the basis for the description of the rheology of a dilute suspension of vesicles without interactions [4,5,14]. In such suspension, theory predicts that the suspension viscosity, η_s, decreases with increasing viscosity contrast, $\lambda = \eta_{in}/\eta_{out}$, and η_{out} fixed, where η_{in} and η_{out} are the inner and the outer fluid viscosities, when the vesicles are driven in the tank-treading (tt) regime of motion. The reduction in η_s occurs due to the tendency of non-spherical vesicles to align with the shear flow in the tt membrane motion. Furthermore, according to a recent theory [14], above some value λ_c, the transition from the tt mode to either the tumbling (tu) or trembling (tr) (also called vacillating-breathing [3] or swinging [15]) motions of single-vesicle dynamics leads to a sharp increase in η_s. In this letter, we present the first experimental study on the interaction of two vesicles of similar sizes and on the influence of the many surrounding vesicles on the dynamics of a single vesicle, and discuss their implications for the rheology of semi-dilute vesicle suspensions.

Experimental setup and methods. – Measurements of vesicle dynamics were conducted in shear flow, in the near-wall region at a half-height of a micro-channel via epi-fluorescent microscopy (see scheme in the fig. 1). The rectangular micro-channels with 380 μm height, 250 μm width were manufactured in an elastomer (PDMS) by a soft lithography [16]. An observation area of $87 \times 66\,\mu\text{m}^2$ was captured by a Mintron MTV-12V1 interlaced CCD camera and digitized via an Ellips Rio frame grabber. A mechanical chopper was synchronized with a CCD camera and installed in the Ar-ion laser beam path, reducing actual exposure time down to ~ 1 ms, which made capturing vesicles with velocity up to hundreds of μm/s possible without noticeable smearing of a vesicle image. The micro-channel could be translated in the direction of the flow via motorized translation stage, for obtaining temporal data in the reference frame associated with a moving vesicle. Control of stepping motor drivers were performed under Labview.

A suspension of deflated vesicles was driven through a micro-channel by a micro-syringe pump at a constant flow rate. The velocity field was measured by the particle tracking velocimetry (PTV) technique with 1 μm fluorescent beads. The idea of the the technique involves firstly, capturing of subsequent images. The second step is the identification of the particles on each image by correlation with a predefined prototype. The last step is the reconstruction of the particle trajectories by joining the position of a particle on subsequent images with further

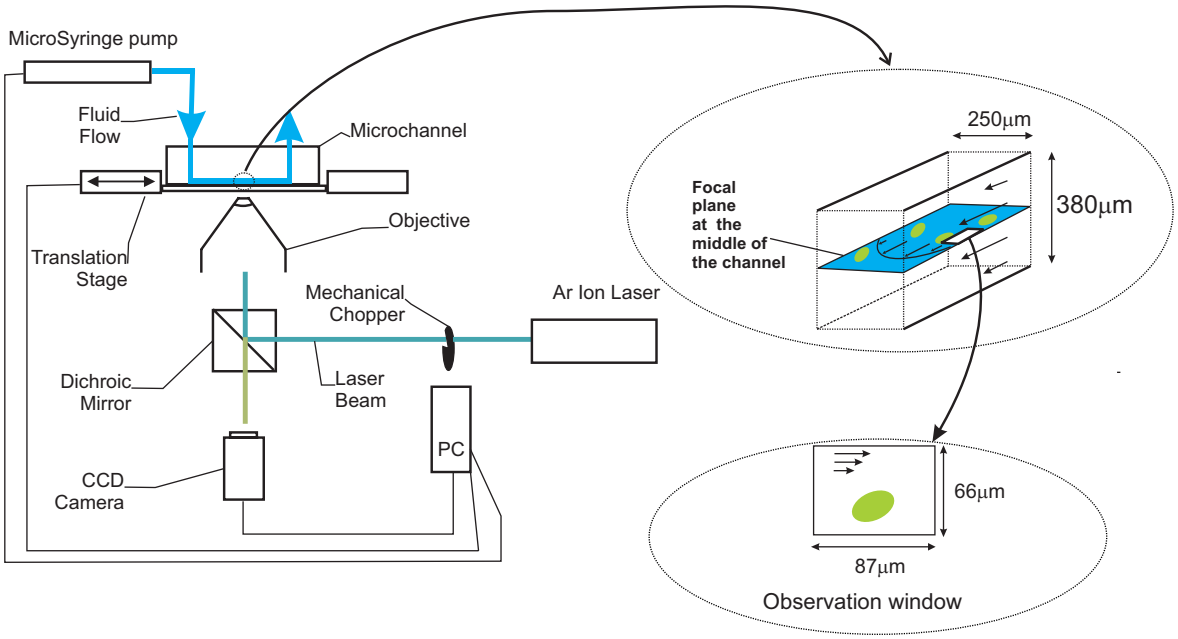

Fig. 1: Experimental setup.

determination velocity field from the given trajectories. The measurements of vesicle dynamics were performed at a distance h between about 5 and 45 μm from the wall. The deviation of the shear rate from a constant was $< \pm 5\%$ on the vesicle size. The lift force, that results in a vesicle drift and shape change [17,18] is negligible. Indeed, simple estimates from ref. [17] give for the ratio of the drift, v_{lift}, and translation, v_{trans}, velocities $v_{lift}/v_{trans} \sim 10(h/R)^3 \sim 10^{-4}$–$10^{-2}$. Thus, it does not introduce any noticeable problem or measurable effects in the results.

Giant unilamellar vesicles were prepared by an electroformation method [19]. The lipid solutions consisted of 85% DOPC (Sigma) and 15% NBD-PC (fluorescent lipid, Molecular Probes) dissolved in either 9 : 1 v/v chloroform-methanol solvent (1.8 mg/ml total lipids), or DOPC in the solvent (1.5 mg/ml). The inner fluid, in which the vesicles were swollen, was either (a) a glucose(monohydrate)-water solution (5.5% w/w) with 500 or 2000 kDa dextran, added to increase the fluid viscosity, (b) sucrose-water (9.3%), or (a)+(b). Viscosity contrasts different from unity and high vesicle concentrations were achieved by gentle centrifugation, which separates the outer medium, and by its replacement by one of the outer fluids: (a), (b) or (a)+(b) added in order to achieve the desired viscosity contrast and to compensate buoyancy. We determine the vesicle volume concentration like done for the hematocrit, that is centrifugating the suspension and measuring the volume ratio between sediment and total. Operative suspensions were produced by "gentle" centrifugation at accelerations $a = 15$–$40\,g$ for 30–60 minutes, causing forces that are necessary to separate vesicles with $R > 3\,\mu$m, but not sufficient to squeeze out completely the solvent from the sediment. The volume ratio measured then is $H' = 15\%$, while the true concentration H of vesicles is expected to be smaller. Expressing $H = (1-\beta)H'$, we determined β experimentally via two additional tests: i) a second sedimentation was carried out at $a = 1000\,g$, resulting in about 100 times larger forces, in order to squeeze out completely the solvent (even if too violent to viable vesicles); ii) separately, we performed repeated gentle separation steps, added each time a highly viscous solvent to the sediment, and measured the viscosity of the liquid residue after centrifugation. The viscosity, measured with about 1% accuracy, is related to the concentration change of the residue and to the amount of original solvent incrementally expelled from the sediment, which are determined with similar accuracy. As a result of these tests, we found $\beta = 0.25 \pm 0.05$ for our preparation procedure, and we used this value throughout. This care provides also a precise determination of λ. The total vesicle volume concentration, H, was 19% for measurements of the vesicle dynamics, and 11.3 and 3.8% for rheology. The rheological measurements were carried out on a viscometer Vilastic-3 and a rheometer Rheolyst AR 1000-N at $22.8 \pm 0.05\,^\circ$C.

Results. – Examples of interactions of two vesicles in the *tt* regime in a shear flow are presented in (figs. 2a,b). Our observations were partially inspired by numerical simulations of interacting drops [20] and capsules [21] in a shear flow. Such cases are however different, as capsules are bounded by a thin elastic membrane capable of sustaining elastic and shear stresses but devoid of bending elasticity, whereas drops are affected by surface tension. For vesicles, the vorticity of the flow keeps the membrane rotating around the inner fluid, during the interaction process. We monitored the relative center-of-mass trajectories (fig. 2c) for several vesicle pairs

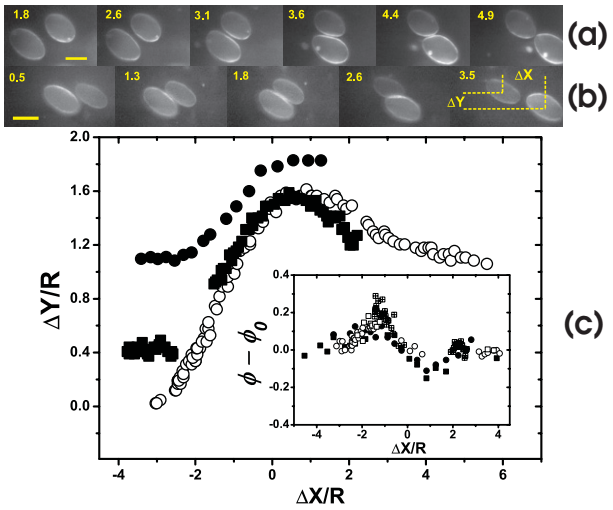

Fig. 2: Snapshots of interacting vesicle pairs with $\lambda = 1$ and $\eta_{out} = 1.3 \cdot 10^{-3}$ Pa·s: (a) $\Delta = 0.3$, $\chi = 39$, and (b) $\Delta = 0.7$, $\chi = 26$. The numbers in the left corners of each image are the normalized times $t\dot{\gamma}$, and the scale bars are 20 μm. (c) Relative vertical displacement of the centers of mass of three vesicle pairs with respect to the common center of mass: full circles for (a), open circles for (b), and squares for vesicles with $\Delta = 0.4$, $\chi = 10$. Inset: deviations of the inclination angle, ϕ, from its average stationary value, ϕ_0, in *tt* motion, *vs.* relative horizontal distance, for data in (c).

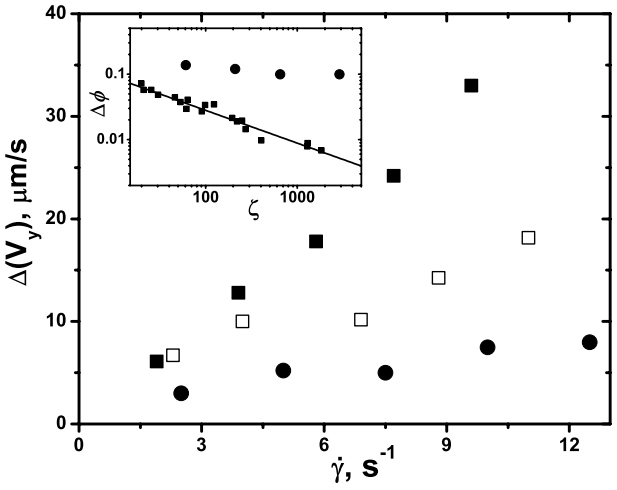

Fig. 3: rms of velocity fluctuations $\Delta(V_y)$ of vesicle suspensions in shear flow, $H \simeq 19\%$, measured by PTV *vs.* $\dot{\gamma}$, circles: solvent (instrumental error due to PTV), full squares: $\lambda = 1$, open squares: $\lambda = 8.6$. Inset: $\Delta\phi$ *vs.* normalized shear rate, ζ; squares: data for dilute suspension from ref. [11] at $\lambda = 1$, circles: data for semi-dilute suspension at $\lambda = 1$. The solid line is the theoretical curve.

with $\lambda = 1$, at different values of the dimensionless shear rate $\chi = \dot{\gamma}\eta_{out}R^3/\kappa$ and the excess area Δ, where $\Delta = S/R^2 - 4\pi$. Here $\dot{\gamma}$ is the shear rate, κ is the membrane bending rigidity, and S and R are, respectively, the total surface area and the effective radius of the vesicle, defined via $V = \frac{4}{3}\pi R^3$. The excess area Δ in the case of *tt* motion was calculated as $\Delta = 32\pi D^2/15$, for deformation parameter $D = \frac{L-B}{L+B}$, where L and B are the small and large semi-axis of the vesicle projection on the shear plane. As in the case of droplets and capsules, deformable vesicles can slide over and around each other with reduced dissipation. This fact implies that, as H increases and vesicle pair interactions become more important, the contribution of each vesicle to the shear stress decreases. As with droplets [20] and capsules [21], the interaction is responsible for a visible deformation of the vesicles at the near-contact position, and causes the vertical separation between the centers of mass to increase after scattering (figs. 2a–c). Moreover, the angular deviations from the average stationary inclinations, ϕ_0, during the scattering are clearly correlated, as presented in the inset of fig. 2c.

As the result of all uncorrelated *tt* membrane motions of the many vesicles in suspension, and of hydrodynamically assisted interactions and direct vesicle scattering, the fluctuations of the vertical component of the flow velocity increase dramatically with $\dot{\gamma}$. This growth may be explained by the proportionality of the *tt* membrane velocity to $\dot{\gamma}$. At smaller λ, the *tt* velocity is larger, so the velocity fluctuations become larger (fig. 3). The velocity fluctuations cause a drastic increase of the rms of the inclination angle fluctuations, $\Delta\phi$, and vesicle shape deformations. Remarkably, $\Delta\phi$ are independent of $\dot{\gamma}$, and can reach values more than an order of magnitude larger than the angle fluctuations due to thermal noise (see inset in fig. 3). We introduce the dimensionless shear rate $\zeta \equiv \chi\kappa\Delta^{1/2}/k_BT$ to compare with results from [11]. The actual values of the shear rate explored in the measurements were $\dot{\gamma} = 1$–$50\,\mathrm{s}^{-1}$. The independence of $\Delta\phi$ from $\dot{\gamma}$ can be explained by the same argument, due to which ϕ_0 is independent of $\dot{\gamma}$: both in the equation for torque balance and in that for torque fluctuations balance, all terms are proportional to $\dot{\gamma}$ (see, *e.g.*, [3]), so that the dependence on $\dot{\gamma}$ cancels out.

We measured the probability distribution function of the inclination angle, ϕ, for vesicles in semi-dilute suspension, from an ensemble of approximately 500 samples. The pdf is found to be Gaussian, like for thermal fluctuations in dilute suspensions. We also found that, in spite of much stronger noise, the dependence of ϕ_0 on Δ at various values of λ in the *tt* regime (averaged over vesicle ensembles) was rather similar to what was obtained for isolated single vesicles [11,12] (see inset in fig. 4). In fig. 4 the critical values of the viscosity contrast, λ_c, at which a transition to *tu* occurs, are presented as a function of Δ, together with our early results [12]. The data presented in fig. 4 was obtained statistically averaging large ensembles for each value of the the viscosity contrast, in the same way as it was done before [12]: 100–500 measurements of $\phi_i(\Delta_i)$ were taken for every viscosity contrast, and the angle was plotted as function of Δ (inset fig. 4), then the trend was extrapolated to $\phi = 0$ in order to obtain the critical Δ for given λ. It is obvious from the plot

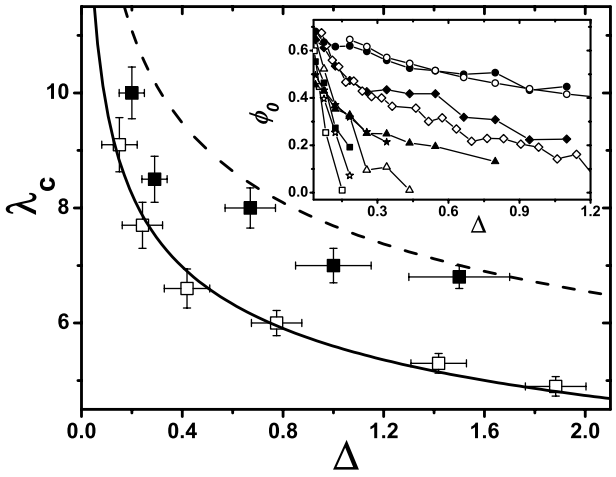

Fig. 4: λ_c *vs.* Δ. Full squares with error bars: data for semi-dilute suspension, $H \simeq 19\%$; the dashed line is the fit $\lambda_c = (\eta_s/\eta_{out})5.6\Delta^{-0.24}$. Open squares with error bars and the fit $\lambda_c = 5.6\Delta^{-0.24}$ are data from [12]. Inset: ϕ_0 *vs.* Δ for several values of λ, circles: 1, rhombus: 4.3, triangles: 6.8, stars: 8, squares: 10; data for non-interacting vesicles, open circles: 1; open rhombus: 4.2, open triangles: 6.6; open stars: 7.7, open squares: 9.1, are taken from [12].

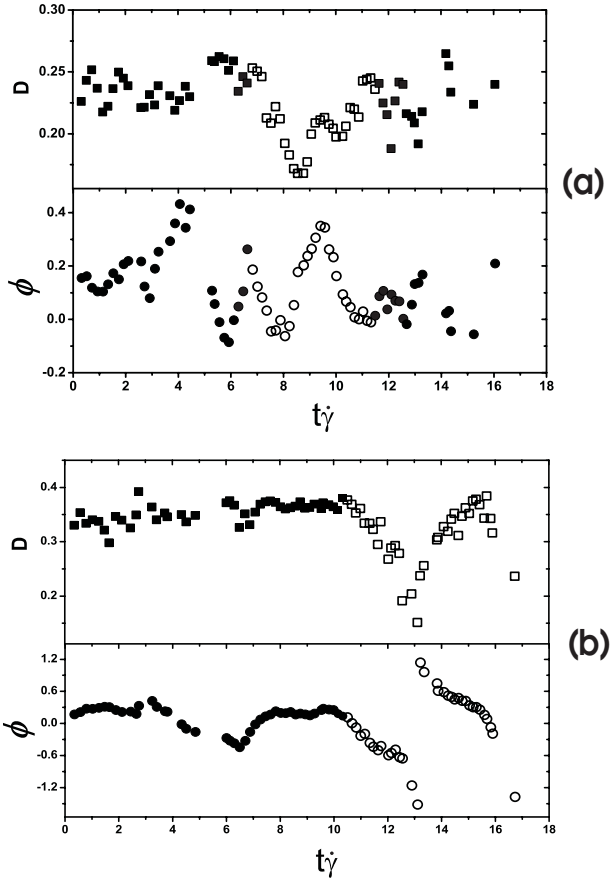

Fig. 5: Dynamics of a single vesicle in a suspension shear flow, $H \simeq 19\%$. (a) squares: D and circles: ϕ *vs.* the reduced time, $t\dot{\gamma}$, for the *tr* regime at $\lambda = 8$ and $\chi = 2.3$; (b) squares: D and circles: ϕ *vs.* $t\dot{\gamma}$, for the *tu* regime at $\lambda = 8$ and $\chi = 0.8$. Open symbols indicate the correlated regions of either *tr* or *tu* dynamics.

that the vesicle interactions postpone the transition to *tu*, though the functional dependence remains the same. Indeed, the dashed curve shown in fig. 4 is obtained by correcting the fitting (solid) curve for the former data [12] by a factor η_s/η_{out}. The corrected fit, however, is about 10% higher than the corresponding current data. Above the transition curve, two types of time-dependent vesicle motions, *tu* and *tr*, were found, as previously observed for isolated vesicles [12]. The difference is that in semi-dilute suspension *tu* and *tr* motions occur randomly in time (see fig. 5). On the other hand, the features of these flipping motions are the same for each event, including the correlations between the shape deformations and the changes in ϕ, while outside the flipping events these variations are not correlated. Thus the dynamics of single vesicles in semi-dilute suspension should be revised taking into account interactions with other vesicles. Both vesicle pair scattering and hydrodynamically assisted interactions in the semi-dilute vesicle suspension enhance considerably vesicle shape and inclination angle fluctuations. However, in spite of the presence of a strong induced noise, the sequence of dynamical states in single-vesicle dynamics as well as the functional dependence of the transition curve remain basically unchanged.

The vesicle interactions and the resulting shape fluctuations become, probably, the intrinsic source of the non-trivial rheology of a semi-dilute suspension, as discussed below. Rheological measurements of suspensions with about $H = 11.3\%$ and 3.8% of vesicles by volume in a wide range of frequencies $f = 0.1$–$2\,\mathrm{s}^{-1}$ and shear rates $\dot{\gamma} = 1$–$50\,\mathrm{s}^{-1}$ show first, that η_s is independent of both the parameters (the inset in fig. 6, data on frequency dependence are not shown), and second, that the storage viscosity, which defines elasticity and relaxation time of a vesicle suspension, is almost equal to or smaller than the resolution of our measurements. Regarding the normal stress in a vesicle suspension, simple estimates in the *tt* regime, based on the theory presented in refs. [5,14], give a maximal value of $N_1 = [3(1 + \Delta/4\pi)\eta_{out}\dot{\gamma}H] \cdot f(\lambda, \Delta) \approx 0.1\,\mathrm{Pa}$, which is smaller than the resolution of our rheometer. Here $f(\lambda, \Delta)$ is defined as in [5], and we used $\lambda = 0.15$ and $\Delta = 0.6$, to compare with the experiment. We thus conclude that the rheological behavior of the semi-dilute vesicle suspension in the *tt* regime is Newtonian within the resolution of our measurements. We found technically almost impossible to run rheological measurements above the transition to *tu* and *tr* regimes, because of the very long time necessary to prepare a sufficient amount of semi-dilute vesicle suspension with $\lambda > 10$.

The viscosity measurements in cone-plate geometry at a constant rotation speed, and in a capillary of 1 mm diameter (Vilastic viscometer) reveal an unexpected non-monotonic dependence on λ of the normalized suspension viscosity, $\tilde{\eta} = (\eta_s/\eta_{out} - 1)/H$, with a change in slope at

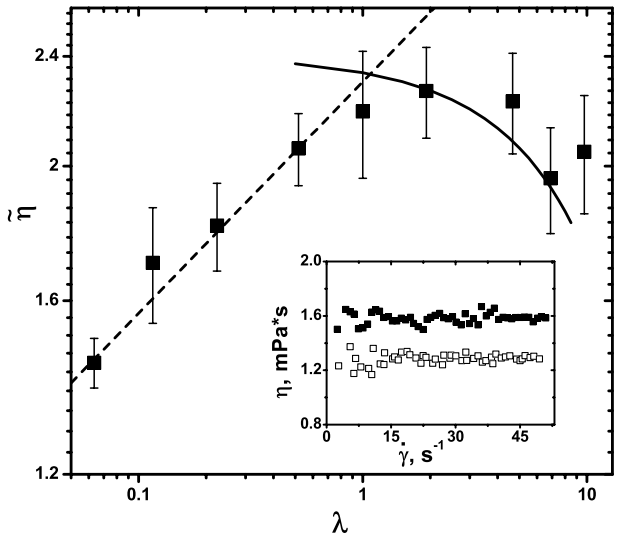

Fig. 6: $\tilde{\eta}$ *vs.* λ: squares with error bars are the data for vesicle concentration $H \simeq 11.3\%$, the dashed curve is the power law fit, $\tilde{\eta} \sim \lambda^{\alpha}$ with $\alpha \approx 1/6$, and the solid curve is the theoretical dependence for dilute vesicle suspensions at $\Delta = 0.15$ [4,5,17]. Inset: dynamic viscosity *vs.* $\dot{\gamma}$ at $\lambda = 7$ for $H \simeq 11.3\%$: open squares: solvent, full squares: suspension.

$\lambda_t \simeq 1$ for $H = 11.3\%$ (fig. 6). Each point on the plot is an average of measurements on several vesicle batches. For $\lambda < 1$, a surprising growth of $\tilde{\eta}$ with λ is observed. The power law fit, $\tilde{\eta} \sim \lambda^{\alpha}$, of the data at $\lambda < 1$ gives $\alpha \approx 1/6$. A similar significant increase of $\tilde{\eta}$ with λ was observed in a shear flow of a concentrated suspension of red blood cells, where the power law dependence with $\alpha \approx 1/4$ was found [22]. At $\lambda > 1$, $\tilde{\eta}$ decreases with λ. The last data point measured at the highest value of $\lambda = 10$ deviates significantly from the declination trend, probably due to the transition to either *tu* or *tr* regimes. Indeed, as pointed out above, *tu* and *tr* dynamics were observed first at $\lambda = 8$ that is rather close to λ_c at $\Delta \simeq 0.6$ (see fig. 4). We also remark that all our viscometric data were obtained on polydisperse samples of vesicle suspensions. Our statistical measurements of vesicle excess areas for several λ, reveal that the mean Δ in *tt* regime varies between 0.2 and 0.6 for different vesicle batches. The viscosity measurements of a suspension with about $H = 3.8\%$ of vesicles by volume were performed for comparison with the $H = 11.3\%$. Error bars were at the level of the mean values in that case, which does not allow to make conclusions about the functional dependence of $\tilde{\eta}$ on λ. Thus, these data confirmed that at least on the current level of resolution of our viscosity measurements it is impossible to test the predictions of theory made for a dilute suspension of vesicle without interactions [4,5,14].

The dependence of $\tilde{\eta}(\lambda)$ we have found even disagrees qualitatively for $\lambda < 1$ with the recent theoretical predictions made for a dilute suspension of vesicles without interactions, according to which $\tilde{\eta}$ almost saturates at $\lambda < 1$ [14,]. This remarkably differs from droplet emulsions, where the theoretical prediction by Taylor [23] on $\tilde{\eta}(\lambda)$ agrees quantitatively with the experiment [24] up to $H = 16\%$. We explain it as follows. In the range of λ under study, a competition between two mechanisms takes part: on the one hand, shape fluctuations due to vesicle interactions lead to larger energy dissipation that causes an increase of $\tilde{\eta}$ with λ; on the other hand, $\tilde{\eta}$ decreases with λ due to alignment of ϕ_0 with the flow direction. Indeed, according to the theory, in a dilute suspension of vesicles without interactions [2,5], at a fixed value of Δ, $\tilde{\eta}$ decreases with increasing λ, due to the better alignment of vesicles with the flow, and therefore with decreasing ϕ_0, which produces a slower *tt* motion of the vesicle membrane. The better alignment of the vesicles with the flow leads to a weaker distortion of the streamlines of the outer flow. In the semi-dilute suspension, for $\lambda < 1$, the viscosity increase due to the enhanced vesicle shape fluctuations outbalances the decrease due to vesicle alignment in shear flow, resulting in the mild increase of $\tilde{\eta}$ with λ. For $\lambda > 1$, the sharper decrease of the viscosity due to the vesicle alignment leads to a declining dependence of $\tilde{\eta}$ on λ. Our results qualitatively agree with the dependence $\tilde{\eta} = 5/2 - \Delta(23\lambda + 32)/16\pi$ with $\Delta = 0.15$ (taken just for illustration purpose) suggested in ref. [4,5,14], as demonstrated in fig. 6. Thus, we infer that for $\lambda > 1$ the second mechanism prevails, resulting finally in the viscosity reduction but with a slower rate than in a dilute suspension of vesicles without interactions [4,5,14].

Conclusions. – To conclude, two unexpected observations are presented in this letter. First, due to long-range hydrodynamic interactions, uncorrelated tank-treading vesicle membrane rotations lead, even in an initially laminar flow, to strong velocity fluctuations that result in strongly enhanced vesicle shape and inclination angle fluctuations. Second, these dynamics of strongly fluctuating vesicles in fluctuating velocity field result in the observed non-trivial, non-monotonic dependence of $\tilde{\eta}$ on λ, which may be ascribed to a competition between vesicle shape fluctuations induced by the vesicle interactions and the vesicle alignment along the flow direction due to the *tt* membrane motion. It is the essential role of the long-range interactions, reflected in $\tilde{\eta}(\lambda)$, that makes the vesicle suspension so different from the droplet emulsion.

* * *

We thank V. Lebedev for helpful remarks and P. Vlahovska for enlightening communications. This work is partially supported by grants from Israel Science Foundation, Binational US-Israel Foundation, Israeli Ministry of Science, Culture and Sport, and by the Minerva Center for Nonlinear Physics of Complex Systems.

REFERENCES

[1] Luisi P. L. and Walde P., *Giant Vesicles* (Wiley, New York) 2000.
[2] Seifert U., *Eur. Phys. J. B*, **8** (1999) 405.

[3] Rioual F., Biben T. and Misbah C., *Phys. Rev. E*, **69** (2004) 061914.
[4] Misbah C., *Phys. Rev. Lett.*, **96** (2006) 028104.
[5] Vlahovska P. and Gracia R., *Phys. Rev. E*, **75** (2007) 016313.
[6] Lebedev V. V., Turitsyn K. S. and Vergeles S. S., *Phys. Rev. Lett.*, **99** (2007) 218101.
[7] Kraus M., Wintz W., Seifert U. and Lipowsky R., *Phys. Rev. Lett.*, **77** (1996) 3685.
[8] Beaucourt J., Rioual F., Seon T., Biben T. and Misbah C., *Phys. Rev. E*, **69** (2004) 011906.
[9] Noguchi H. and Gompper G., *Phys. Rev. Lett.*, **93** (2004) 258102; *Phys. Rev. E*, **72** (2005) 011901.
[10] de Haas K., Bloom C., van den Ende D., Duits M. and Mellema J., *Phys. Rev. E*, **56** (1997) 7132.
[11] Kantsler V. and Steinberg V., *Phys. Rev. Lett.*, **95** (2005) 258101.
[12] Kantsler V. and Steinberg V., *Phys. Rev. Lett.*, **96** (2006) 036001.
[13] Mader M., Vitkova V., Abkarian M., Viallat A. and Podgorski T., *Eur. Phys. J.*, **19** (2006) 389.
[14] Danker G. and Misbah C., *Phys. Rev. Lett.*, **98** (2007) 088104.
[15] Noguchi H. and Gompper G., *Phys. Rev. Lett.*, **97** (2007) 128103.
[16] Xia Y. N. and Whitesides G. M., *Annu. Rev. Mater. Sci.*, **28** (1998) 153.
[17] Abkarian M., Lartigue C. and Viallat A., *Phys. Rev. Lett.*, **88** (2002) 068103.
[18] Sukumaran S. and Seifert U., *Phys. Rev. E*, **64** (2001) 011916.
[19] Angelova M. I., Soleau S., Meleard P., Faucon J.-F. and Bothorel P., *Prog. Colloid Polym. Sci.*, **89** (1992) 127.
[20] Loewenberg M. and Hinch E. J., *J. Fluid Mech.*, **338** (1997) 299.
[21] Lac E., Morel A. and Barthes-Biesel D., *J. Fluid Mech.*, **573** (2007) 149.
[22] Chien S., *Present State of Blood Rheology*, in *Hemodilution, Theoretical Basis and Clinical Application*, edited by Messmer K. and Schmid-Schoenbein H. (Karger, Basel) 1972, p. 1.
[23] Taylor G. I., *Proc. R. Soc. London, Ser. A*, **138** (1932) 41.
[24] Nawab M. and Mason S., *Trans. Faraday Soc.*, **54** (1958) 1712.